Plug-and-Play Tensor Low-Rank Approximation for Hyperspectral Anomaly Detection

Xianchao Xiu

Department of Automation

上海大学
Shanghai University

Algorithm Software and Applications, December 8-10, 2023

Joint work with Jingjing Liu (SHU), Jianhua Zhang (SHU) and others

Outline

HAD

- Hyperspectral anomaly detection (HAD): find abnormal targets, such as infected trees in forests, rare minerals in geosciences, and airplanes in defense

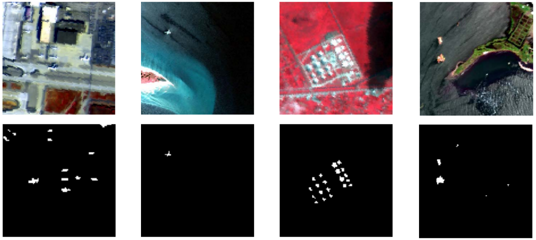

- Benchmark methods (2005-2022)

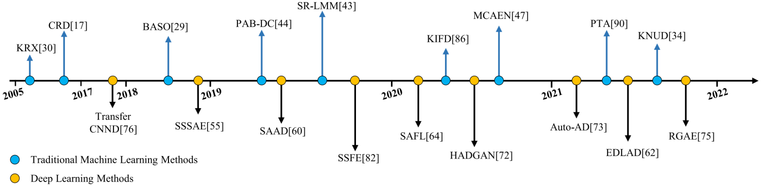

Tensor LRR

- From LRR to TLRR or TLRA

$$\min_{Z,E} \quad \|Z\|_* + \lambda\|E\|_1 \qquad \Rightarrow \qquad \min_{\mathcal{Z},\mathcal{E}} \quad \|\mathcal{Z}\|_{\mathrm{TNN}} + \lambda\|\mathcal{E}\|_1$$

$$\text{s.t.} \quad X = AZ + E \qquad\qquad \text{s.t.} \quad \mathcal{X} = \mathcal{A} * \mathcal{Z} + \mathcal{E}$$

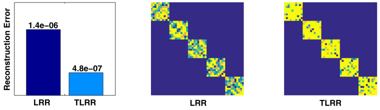

(a) Results of LRR and TLRR on the data with vector linear relations.

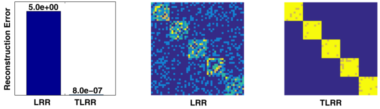

(b) Results of LRR and TLRR on the data with tensor linear relations.

- What are the advantages of tensor modeling?
  - Excellent data representation with (possibly) low computational complexity
  - Different tensor decomposition including Tucker, CP, t-SVD, BT, TT, TR

Tensor LRR

- Wang-Wang-Hong-Roy-Chanussot, IEEE Transactions on Cybernetics, 2023

$$\min_{\mathcal{Z},\mathcal{E}} \ \|\mathcal{Z}\|_{\mathrm{TNN}} + \lambda\|\mathcal{E}\|_1 \quad \text{s.t.} \ \mathcal{X} = \mathcal{A} * \mathcal{Z} + \mathcal{E} \quad \Rightarrow \quad \min_{\mathcal{Z},\mathcal{E}} \ \|\mathcal{Z}\|_{\mathrm{WTNN}} + \lambda\|\mathcal{E}\|_1 \quad \text{s.t.} \ \mathcal{X} = \mathcal{A} * \mathcal{Z} + \mathcal{E}$$

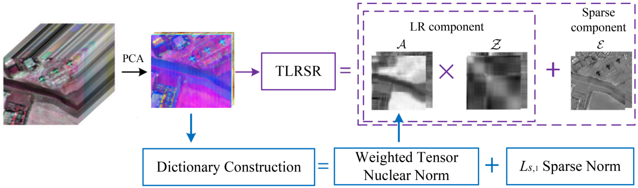

- In this talk, we focus on the following questions
  - How to characterize sparsity?
  - How to integrate deep priors?

Outline

Motivation

- How to characterize sparsity?

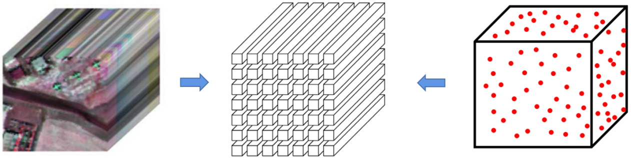

  - Entry-wise sparsity

$$\|\mathcal{E}\|_1 = \sum_{i=1}^{h}\sum_{j=1}^{v}\sum_{k=1}^{z} |\mathcal{E}(i,j,k)| \qquad \Rightarrow \qquad \|\mathcal{E}\|_0 = \sharp\{(i,j,k) \mid |\mathcal{E}(i,j,k)| \neq 0\}$$

  - Tube-wise sparsity

$$\|\mathcal{E}\|_{\mathrm{F},0} = \sharp\{(i,j) \mid \|\mathcal{E}(i,j,:)\|_2 \neq 0\}$$

Motivation

- How to integrate deep priors?

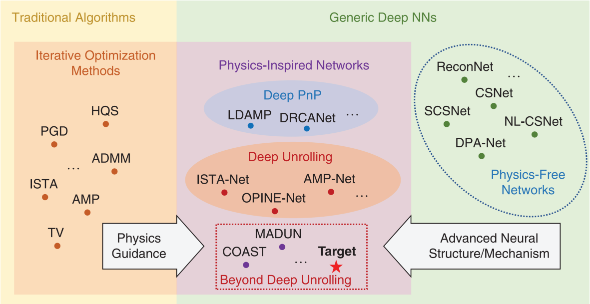

- What are the advantages of PnP modeling?
  - Implicit regularizer yet flexible
  - Learn priors by pre-trained neural networks

Formulation

- Plug-and-play tensor low-rank approximation (PnP-TLRA)

$$\begin{aligned} \min_{\mathcal{Z},\mathcal{E}} \quad & \|\mathcal{Z}\|_{\mathrm{WTNN}} + \lambda\|\mathcal{E}\|_1 \\ \text{s.t.} \quad & \mathcal{X} = \mathcal{A} * \mathcal{Z} + \mathcal{E} \end{aligned}$$

$$\Downarrow$$

$$\begin{aligned} \min_{\mathcal{Z},\mathcal{E},\mathcal{N}} \quad & \|\mathcal{Z}\|_{\mathrm{WTNN}} + \lambda\|\mathcal{E}\|_{\mathrm{F},0} + \mu\|\mathcal{N}\|_{\mathrm{F}}^2 \\ \text{s.t.} \quad & \mathcal{X} = \mathcal{A} * \mathcal{Z} + \mathcal{E} + \mathcal{N} \end{aligned}$$

$$\Downarrow$$

$$\begin{aligned} \min_{\mathcal{Z},\mathcal{E},\mathcal{N}} \quad & \phi(\mathcal{Z}) + \lambda\|\mathcal{E}\|_{\mathrm{F},0} + \mu\|\mathcal{N}\|_{\mathrm{F}}^2 \\ \text{s.t.} \quad & \mathcal{X} = \mathcal{A} * \mathcal{Z} + \mathcal{E} + \mathcal{N} \end{aligned}$$

- $\phi(\mathcal{Z})$: PnP prior ranging from WTNN, nonlinear TNN to DnCNN, FFDNet

Algorithm

- Alternating direction method of multipliers (ADMM)

$$
\begin{aligned}
L_\beta(\mathcal{Z},\mathcal{E},\mathcal{N},\mathcal{Y}) &= \phi(\mathcal{Z}) + \lambda\|\mathcal{E}\|_{\mathrm{F},0} + \mu\|\mathcal{N}\|_{\mathrm{F}}^2 \\
&\quad - \langle \mathcal{Y}, \mathcal{X} - \mathcal{A} * \mathcal{Z} - \mathcal{E} - \mathcal{N}\rangle + \frac{\beta}{2}\|\mathcal{X} - \mathcal{A} * \mathcal{Z} - \mathcal{E} - \mathcal{N}\|_{\mathrm{F}}^2
\end{aligned}
$$

- The iterative scheme
  - Update $\mathcal{Z}^{k+1} = \arg\min_{\mathcal{Z}} \ \phi(\mathcal{Z}) + \frac{\beta}{2}\|\mathcal{X} - \mathcal{A} * \mathcal{Z} - \mathcal{E}^k - \mathcal{N}^k - \mathcal{Y}^k/\beta\|_{\mathrm{F}}^2$
  - Update $\mathcal{E}^{k+1} = \arg\min_{\mathcal{E}} \ \lambda\|\mathcal{E}\|_{\mathrm{F},0} + \frac{\beta}{2}\|\mathcal{X} - \mathcal{A} * \mathcal{Z}^{k+1} - \mathcal{E} - \mathcal{N}^k - \mathcal{Y}^k/\beta\|_{\mathrm{F}}^2$
  - Update $\mathcal{N}^{k+1} = \arg\min_{\mathcal{N}} \ \mu\|\mathcal{N}\|_{\mathrm{F}}^2 + \frac{\beta}{2}\|\mathcal{X} - \mathcal{A} * \mathcal{Z}^{k+1} - \mathcal{E}^{k+1} - \mathcal{N} - \mathcal{Y}^k/\beta\|_{\mathrm{F}}^2$
  - Update $\mathcal{Y}^{k+1} = \mathcal{Y}^k - \beta(\mathcal{X} - \mathcal{A} * \mathcal{Z}^{k+1} - \mathcal{E}^{k+1} - \mathcal{N}^{k+1})$
- Update $\mathcal{Z}$ via solving

$$
\min_{\mathcal{Z}} \ \phi(\mathcal{Z}) + \langle \nabla_{\mathcal{Z}} g(\mathcal{Z}^k), \mathcal{Z} - \mathcal{Z}^k\rangle + \frac{\eta}{2}\|\mathcal{Z} - \mathcal{Z}^k\|_{\mathrm{F}}^2
$$

  - Consider $\phi(\mathcal{Z}) = \|\mathcal{Z}\|_{\mathrm{WTNN}}$, then $\mathcal{Z}^{k+1} = \mathrm{Shrink}_{\mathcal{W}^k}(\mathcal{Z}^k - \nabla_{\mathcal{Z}} g(\mathcal{Z}^k)/\eta, 1/\eta)$
  - Consider $\phi(\mathcal{Z}) = \|\mathcal{Z}\|_{\mathrm{FFDNet}}$, then $\mathcal{Z}^{k+1} = \mathrm{FFDNet}(\mathcal{Z}^k - \nabla_{\mathcal{Z}} g(\mathcal{Z}^k)/\eta, 1/\eta)$

Convergence

Lemma (decreasing)

The generated sequence $\{L_\beta(\mathcal{Z}^k, \mathcal{E}^k, \mathcal{N}^k, \mathcal{Y}^k)\}$ *is decreasing.*

Lemma (boundedness)

A generated sequence $\{(\mathcal{Z}^k, \mathcal{E}^k, \mathcal{N}^k, \mathcal{Y}^k)\}$ *is bounded.*

Theorem (subsequential convergence)

Any cluster point $\{\mathcal{Z}^*, \mathcal{E}^*, \mathcal{N}^*, \mathcal{Y}^*\}$ *converges to a stationary point of TLRA.*

Theorem (global convergence)

With the assumption of KL function, the sequence $\{(\mathcal{Z}^k, \mathcal{E}^k, \mathcal{N}^k, \mathcal{Y}^k)\}$ *converges to a stationary point of TLRA.*

Note that additional assumptions are required for PnP-TLRA!

Experiments

- Datasets: San Diego, HYDICE, Indian Pines, ABU (airport, beach, urban)
- Compared methods: matrix/tensor
  - RPCA-RX: Low-Rank and Sparse Matrix Decomposition-Based Anomaly Detection for Hyperspectral Imagery, 2019
  - LSMAD: A Low-Rank and Sparse Matrix Decomposition-Based Mahalanobis Distance Method for Hyperspectral Anomaly Detection, 2015
  - LRASR: Anomaly Detection in Hyperspectral Images Based on Low-Rank and Sparse Representation, 2016
  - GTVLRR: Graph and Total Variation Regularized Low-Rank Representation for Hyperspectral Anomaly Detection, 2020
  - ELRSF-SP: Hyperspectral Anomaly Detection via Enhanced Low-Rank and Smoothness Fusion Regularization Plus Saliency Prior, 2024
  - TPCA: A Preprocessing Method for Hyperspectral Target Detection Based on Tensor Principal Component Analysis, 2018
  - PTA: Prior-Based Tensor Approximation for Anomaly Detection in Hyperspectral Imagery, 2022
  - PCA-TLRSR: Learning Tensor Low-Rank Representation for Hyperspectral Anomaly Detection, 2023

Experiments

- Area under the curve (AUC)

Dataset	GRXD	RPCA-RX	LSMAD	GTVLRR	TPCA	PTA	PCA-TLRSR	GAED	GNLTR	ELRSF-SP	TLRA	PnP-TLRA
SD	0.8886	0.9165	0.9457	0.9648	0.8849	0.9868	0.9923	0.9889	0.9838	0.9878	0.9927	**0.9942**
HYDICE	0.9857	0.9842	0.9906	0.9918	0.8242	0.8396	0.9802	0.9639	0.9859	0.9768	0.9840	**0.9968**
ABU-airport-1	0.8221	0.8089	0.8341	0.8957	0.8023	0.7698	0.9291	0.8106	0.9293	0.8221	**0.9331**	0.9303
ABU-airport-2	0.8403	0.8431	0.9192	0.8911	0.8891	0.8995	0.9345	0.9272	0.9242	0.8891	0.9409	**0.9523**
ABU-airport-3	0.9288	0.9275	0.9398	0.9287	0.9297	0.7369	0.9233	0.8638	0.9330	0.9209	0.9379	**0.9380**
ABU-airport-4	0.9526	0.9627	0.9864	0.9776	0.9432	0.9890	0.9914	0.9654	0.9606	0.9876	**0.9932**	0.9918
ABU-beach-1	0.9804	0.9761	0.9778	0.9703	0.9860	0.9682	0.9831	0.9223	0.9638	0.9780	0.9868	**0.9895**
ABU-beach-2	0.9106	0.9097	0.9056	0.9348	0.8061	0.8862	0.9331	0.5061	0.9472	0.9097	**0.9580**	0.9533
ABU-beach-3	**0.9998**	0.9995	0.9996	0.9866	0.9982	0.9483	0.9994	0.9891	0.9928	0.9945	0.9994	0.9996
ABU-beach-4	0.9538	0.9599	0.9349	0.9803	0.9338	0.9000	0.9755	0.8514	0.9044	0.9698	0.9899	**0.9902**
ABU-urban-1	0.9907	0.9922	0.9818	0.8742	0.9390	0.8940	0.9923	0.9409	0.9325	0.9907	0.9934	**0.9951**
ABU-urban-2	0.9946	0.9957	0.9849	0.8628	0.9409	0.9701	0.9928	0.9958	0.9874	0.9946	0.9983	**0.9994**
ABU-urban-3	0.9513	0.9577	0.9633	0.9365	0.8224	0.9090	0.9832	0.9725	0.9667	0.9513	**0.9888**	0.9855
ABU-urban-4	0.9887	0.9871	0.9809	0.9205	0.9835	0.9937	0.9857	0.9556	0.9931	0.9909	0.9883	**0.9950**
ABU-urban-5	0.9690	0.9658	0.9610	0.9347	0.9370	0.8693	0.9811	0.9148	0.9297	0.9658	0.9821	**0.9837**
Average	0.9438	0.9458	0.9537	0.9367	0.9080	0.9040	0.9718	0.9046	0.9556	0.9553	0.9778	**0.9796**

Experiments

- Receiver operating characteristic (ROC)

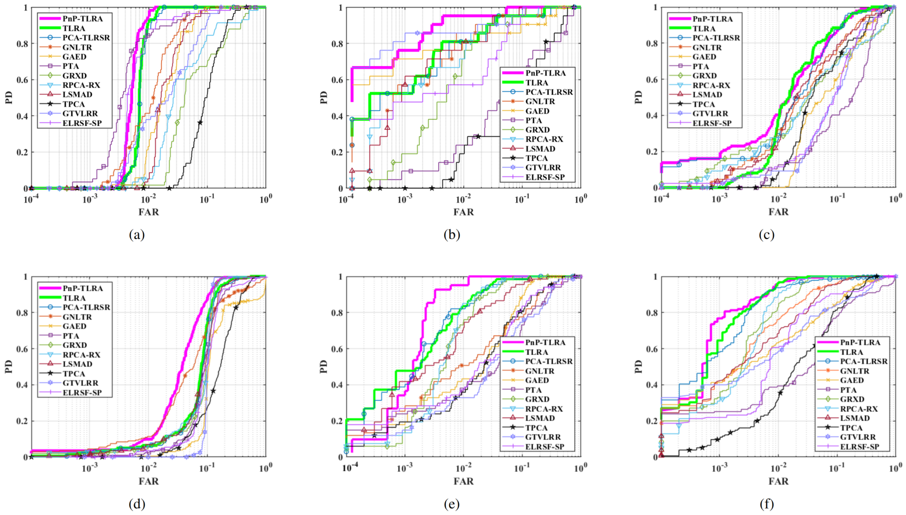

Experiments

- Results on the San Diego dataset

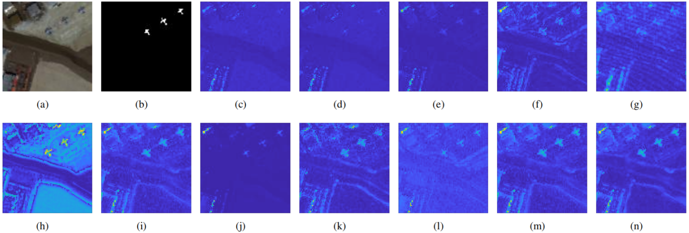

- Results on the HYDICE dataset

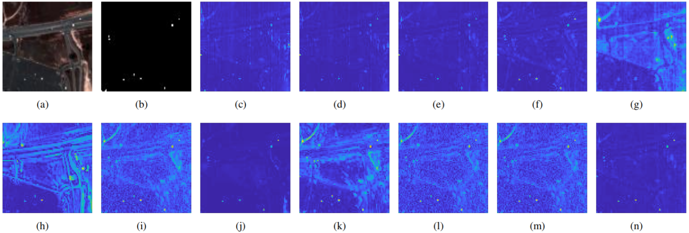

Experiments

- Statistical separability analysis

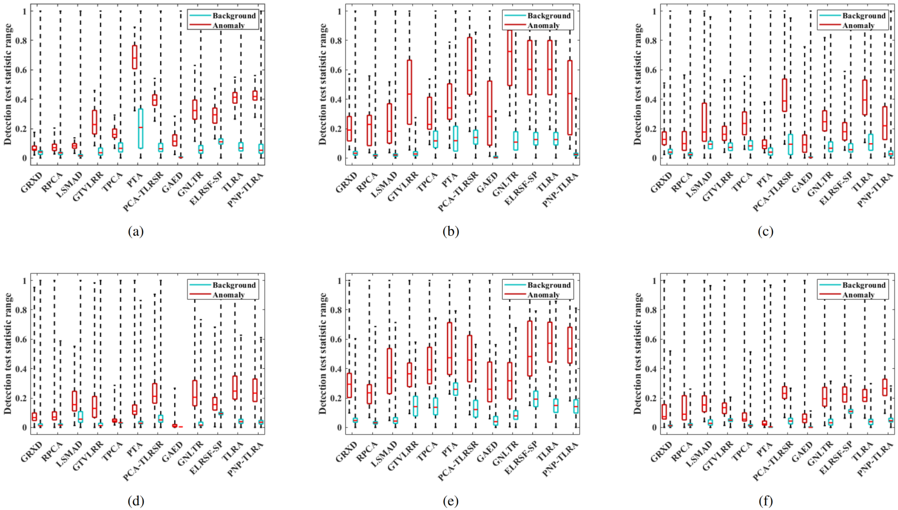

Experiments

- Noise robustness

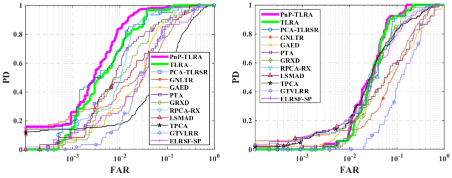

(a) SNR=12.64 dB (b) SNR=5.43 dB

SNR (dB)	GRXD	RPCA-RX	LSMAD	GTVLRR	TPCA	PTA
Original	0.9907	0.9922	0.9817	0.8742	0.9390	0.8940
12.64	0.9431	0.9474	0.9378	0.8548	0.9097	0.8548
5.43	0.9089	0.9044	0.8991	0.8221	0.8608	0.8364

SNR (dB)	PCA-TLRSR	GAED	GNLTR	ELRSF-SP	TLRA	PnP-TLRA
Original	0.9923	0.9409	0.9325	0.9907	0.9934	**0.9951**
12.64	0.9505	0.9209	0.9059	0.9389	0.9513	**0.9577**
5.43	0.9106	0.8840	0.8721	0.9027	0.9171	**0.9199**

- Runtime comparisions

Dataset	TPCA	PTA	PCA-TLRSR	TLRA	PnP-TLRA
San Diego	34.66	26.37	10.99	**5.89**	10.63
HYDICE	25.39	22.76	9.31	**4.89**	24.49
ABU-airport	41.63	29.21	11.32	**6.12**	9.71
ABU-beach	29.04	38.24	15.61	**10.86**	12.31
ABU-urban	36.95	28.01	17.35	**8.38**	11.82

Outline

Motivation

- Weighted multidirectional sparsity (WMS)

$$\|E\|_1 = \sum_{i=1}^{m}\sum_{j=1}^{n}|E(i,j)|$$

$$\Downarrow$$

$$\Omega(E) = \sum_{j=1}^{n}\sum_{g\in\mathcal{G}}\|e_g^j\|_\infty$$

$$\Downarrow$$

$$\Omega(\mathcal{E}) = \sum_{i=1}^{3} w_i \texttt{fold}(\Omega(\texttt{unfold}(\mathcal{E}, i)), i)$$

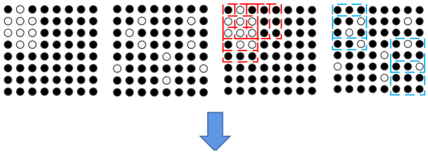

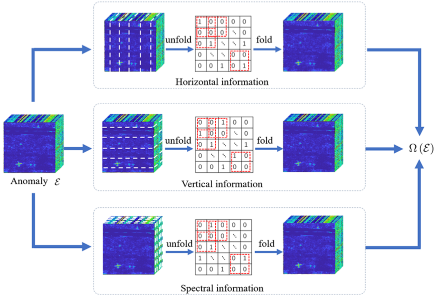

Formulation

- WMS regularized low-rank tensor representation (WMS-LRTR)

$$\min_{\mathcal{Z},\mathcal{E}} \ \|\mathcal{Z}\|_{\mathrm{WTNN}} + \lambda\|\mathcal{E}\|_1$$
$$\text{s.t.} \ \ \mathcal{X} = \mathcal{A} * \mathcal{Z} + \mathcal{E}$$

$$\Downarrow$$

$$\min_{\mathcal{Z},\mathcal{E}} \ \|\mathcal{Z}\|_{\mathrm{WTNN}} + \lambda\Omega(\mathcal{E})$$
$$\text{s.t.} \ \ \mathcal{X} = \mathcal{A} * \mathcal{Z} + \mathcal{E}$$

$$\Downarrow$$

$$\min_{\mathcal{Z},\mathcal{E}} \ \|\mathcal{Z}\|_{\mathrm{WTNN}} + \lambda\Omega(\mathcal{E}) + \mu\phi(\mathcal{E})$$
$$\text{s.t.} \ \ \mathcal{X} = \mathcal{A} * \mathcal{Z} + \mathcal{E}$$

- $\phi(\mathcal{E})$: PnP denoiser including BM4D, WNNM, FFDNet, SwinIR

Algorithm

- Alternating direction method of multipliers (ADMM)

$$\begin{aligned} \min_{\mathcal{Z},\mathcal{E},\mathcal{Y},\mathcal{W}} \quad & \|\mathcal{Z}\|_{\mathrm{WTNN}} + \lambda\Omega(\mathcal{E}) + \mu\phi(\mathcal{Y}) \\ \text{s.t.} \quad & \mathcal{X} = \mathcal{A} * \mathcal{W} + \mathcal{E},\ \mathcal{Z} = \mathcal{W},\ \mathcal{Y} = \mathcal{E} \end{aligned}$$

$$\Downarrow$$

$$\begin{aligned} L_\beta(\mathcal{Z},\mathcal{E},\mathcal{Y},\mathcal{W},\mathcal{Q}_1,\mathcal{Q}_2,\mathcal{Q}_3) &= \|\mathcal{Z}\|_{\mathrm{WTNN}} + \lambda\Omega(\mathcal{E}) + \mu\phi(\mathcal{Y}) \\ &+ \langle \mathcal{Q}_1, \mathcal{X} - \mathcal{A} * \mathcal{W} - \mathcal{E}\rangle + \frac{\beta}{2}\|\mathcal{X} - \mathcal{A} * \mathcal{W} - \mathcal{E}\|_{\mathrm{F}}^2 \\ &+ \langle \mathcal{Q}_2, \mathcal{Z} - \mathcal{W}\rangle + \frac{\beta}{2}\|\mathcal{Z} - \mathcal{W}\|_{\mathrm{F}}^2 + \langle \mathcal{Q}_3, \mathcal{Y} - \mathcal{E}\rangle + \frac{\beta}{2}\|\mathcal{Y} - \mathcal{E}\|_{\mathrm{F}}^2 \end{aligned}$$

- Two issues should be considered
  - How to update $\mathcal{E}$ $\Rightarrow$ Quadratic min-cost flow
  - How to construct dictionary $\Rightarrow$ PCA

$$\min_{\mathcal{L},\mathcal{S}} \|\mathcal{L}\|_{\mathrm{WTNN}} + \alpha\Omega(\mathcal{S}) \quad \text{s.t.} \quad \mathcal{X} = \mathcal{L} + \mathcal{S}$$

Experiments

- Datasets: ABU (airport, beach, urban)
- Compared methods: machine learning/deep learning
  - LRASR: Anomaly Detection in Hyperspectral Images Based on Low-Rank and Sparse Representation, 2016
  - GTVLRR: Graph and Total Variation Regularized Low-Rank Representation for Hyperspectral Anomaly Detection, 2020
  - PTA: Prior-Based Tensor Approximation for Anomaly Detection in Hyperspectral Imagery, 2022
  - PCA-TLRSR: Learning Tensor Low-Rank Representation for Hyperspectral Anomaly Detection, 2023
  - LARTVAD: Hyperspectral Anomaly Detection With Tensor Average Rank and Piecewise Smoothness Constraints, 2023
  - DeCNN-AD: Hyperspectral Anomaly Detection via Deep Plug-and-Play Denoising CNN Regularization, 2021
  - Auto-AD: Autonomous Hyperspectral Anomaly Detection Network Based on Fully Convolutional Autoencoder, 2022
  - RGAE: Hyperspectral Anomaly Detection With Robust Graph Autoencoders, 2022

Experiments

- AUC values on the Airport scenes

Dataset	AUC	RX	LRASR	GTVLRR	AUTO-AD	RGAE	DeCNN-AD	PTA	PCA-TLRSR	LARTVAD	WMS-LRTR
Airport-1	$AUC_{(D,F)}\uparrow$	0.8221	0.7284	0.8997	0.6941	0.6387	0.8662	0.9109	0.9420	0.9202	**0.9435**
	$AUC_{(D,\tau)}\uparrow$	0.0987	0.1711	0.2665	0.1595	0.0506	0.1562	**0.3471**	0.3088	0.2540	0.3284
	$AUC_{(F,\tau)}\downarrow$	0.0424	0.1209	0.1153	0.0991	**0.0255**	0.0689	0.1191	0.0918	0.0816	0.1001
	$AUC_{TD}\uparrow$	0.9208	0.8996	1.1647	0.8536	0.6889	1.0224	1.2580	1.2508	1.1742	**1.2718**
	$AUC_{BS}\uparrow$	0.7797	0.6075	0.7844	0.5950	0.6128	0.7974	0.7918	**0.8502**	0.8386	0.8433
	$AUC_{TDBS}\uparrow$	0.0563	0.0502	0.1496	0.0603	0.0252	0.0873	0.2279	0.2170	0.1724	**0.2282**
	$AUC_{ODP}\uparrow$	0.8784	0.7786	1.0493	0.7544	0.6635	0.9536	1.1388	1.1590	1.0927	**1.1717**
Airport-2	$AUC_{(D,F)}\uparrow$	0.8403	0.8707	0.8670	0.6764	0.7470	0.9656	0.9411	0.9543	0.9387	**0.9704**
	$AUC_{(D,\tau)}\uparrow$	0.1841	0.3156	0.3175	0.1976	0.0770	0.3257	**0.4334**	0.3705	0.2845	0.3807
	$AUC_{(F,\tau)}\downarrow$	0.0516	0.1613	0.1379	0.0862	**0.0196**	0.0476	0.1292	0.0753	0.0692	0.0652
	$AUC_{TD}\uparrow$	1.0245	1.1863	1.1845	0.8439	0.8239	1.2913	**1.3745**	1.3248	1.2233	1.3511
	$AUC_{BS}\uparrow$	0.7888	0.7094	0.7291	0.5902	0.7274	**0.9180**	0.8119	0.8790	0.8696	0.9052
	$AUC_{TDBS}\uparrow$	0.1325	0.1542	0.1797	0.0814	0.0574	0.2781	0.3042	0.2952	0.2154	**0.3155**
	$AUC_{ODP}\uparrow$	0.9709	1.0249	1.0467	0.7578	0.8044	1.2437	1.2453	1.2495	1.1541	**1.2859**
Airport-3	$AUC_{(D,F)}\uparrow$	0.9288	0.9234	0.9231	0.9210	0.8873	0.9235	0.9247	0.9540	0.8877	**0.9579**
	$AUC_{(D,\tau)}\uparrow$	0.0660	0.0562	0.0695	0.1278	0.0511	0.0676	**0.1665**	0.1398	0.1203	0.1333
	$AUC_{(F,\tau)}\downarrow$	0.0145	0.0126	0.0155	0.0395	**0.0057**	0.0123	0.0416	0.0279	0.0326	0.0194
	$AUC_{TD}\uparrow$	0.9948	0.9796	0.9927	1.0488	0.9384	0.9916	1.0911	**1.0945**	1.0080	1.0912
	$AUC_{BS}\uparrow$	0.9144	0.9108	0.9077	0.8815	0.8816	0.9117	0.8831	0.9268	0.8551	**0.9385**
	$AUC_{TDBS}\uparrow$	0.0516	0.0436	0.0540	0.0883	0.0454	0.0553	**0.1249**	0.1119	0.0877	0.1139
	$AUC_{ODP}\uparrow$	0.9804	0.9670	0.9772	1.0094	0.9327	0.9793	1.0496	1.0666	0.9754	**1.0718**
Airport-4	$AUC_{(D,F)}\uparrow$	0.9526	0.9566	0.9836	0.9840	0.7508	0.9239	0.9841	0.9933	0.9173	**0.9961**
	$AUC_{(D,\tau)}\uparrow$	0.0736	0.3747	0.4437	0.4071	0.1172	0.4229	**0.6476**	0.4350	0.0931	0.5110
	$AUC_{(F,\tau)}\downarrow$	**0.0248**	0.1053	0.0942	0.0267	0.0749	0.1646	0.1044	0.0924	0.0311	0.0427
	$AUC_{TD}\uparrow$	1.0262	1.3313	1.4273	1.3911	0.8679	1.3467	**1.6317**	1.4283	1.0104	1.5071
	$AUC_{BS}\uparrow$	0.9278	0.8513	0.8894	**0.9573**	0.6759	0.7593	0.8798	0.9008	0.8862	0.9534
	$AUC_{TDBS}\uparrow$	0.0489	0.2693	0.3496	0.3804	0.0423	0.2583	**0.5432**	0.3426	0.0620	0.4684
	$AUC_{ODP}\uparrow$	1.0015	1.2260	1.3332	1.3644	0.7930	1.1822	**1.5273**	1.3358	0.9793	1.4645

Experiments

- ROC curves on the Airport-1 dataset

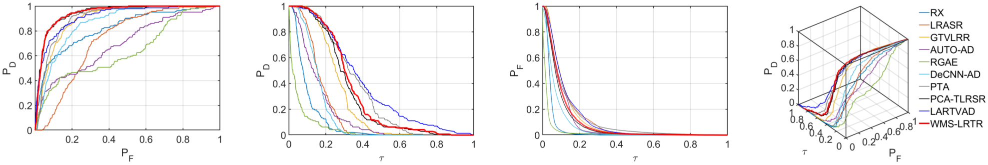

- ROC curves on the Airport-2 dataset

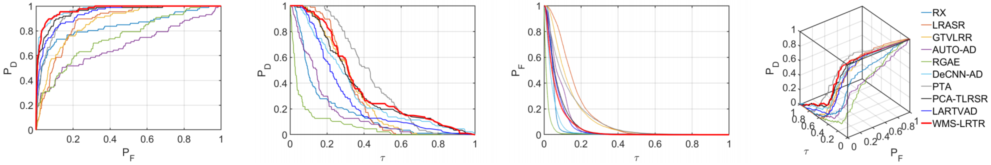

Experiments

- Noise robustness

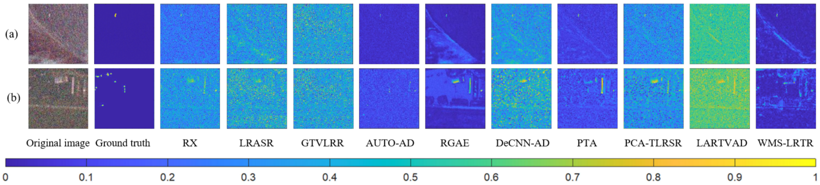

Dataset	AUC	RX	LRASR	GTVLRR	AUTO-AD	RGAE	DeCNN-AD	PTA	PCA-TLRSR	LARTVAD	WMS-LRTR
Noisy Beach-3	$AUC_{(D,F)} \uparrow$	0.9267	0.7543	0.6208	0.7905	0.8067	0.7806	0.9740	0.8109	0.8602	**0.9755**
	$AUC_{(D,\tau)} \uparrow$	0.5386	0.5523	0.5122	0.2924	0.3427	0.5665	0.5110	0.5785	**0.7330**	0.4833
	$AUC_{(F,\tau)} \downarrow$	0.2453	0.3667	0.4267	0.0607	0.0630	0.3506	0.1056	0.3105	0.5712	**0.0491**
	$AUC_{TD} \uparrow$	1.4652	1.3066	1.1330	1.0829	1.1494	1.3470	1.4850	1.3894	**1.5932**	1.4589
	$AUC_{BS} \uparrow$	0.6814	0.3876	0.1941	0.7297	0.7437	0.4300	0.8684	0.5004	0.2889	**0.9264**
	$AUC_{TDBS} \uparrow$	0.2933	0.1856	0.0854	0.2316	0.2797	0.2158	0.4054	0.2680	0.1618	**0.4342**
	$AUC_{ODP} \uparrow$	1.2200	0.9400	0.7063	1.0221	1.0864	0.9964	1.3794	1.0790	1.0220	**1.4097**
Noisy Urban-3	$AUC_{(D,F)} \uparrow$	0.6873	0.5919	0.5124	0.6794	0.4518	0.5492	0.9085	0.6180	0.6893	**0.9281**
	$AUC_{(D,\tau)} \uparrow$	0.4440	0.4611	0.4061	0.2357	0.0781	0.4445	0.3519	0.4470	**0.6803**	0.2803
	$AUC_{(F,\tau)} \downarrow$	0.3539	0.4127	0.3971	0.1358	0.0955	0.4177	0.1543	0.3956	0.6219	**0.0714**
	$AUC_{TD} \uparrow$	1.1312	1.0530	0.9185	0.9151	0.5299	0.9937	1.2604	1.0650	**1.3696**	1.2084
	$AUC_{BS} \uparrow$	0.3334	0.1791	0.1153	0.5436	0.3563	0.1315	0.7541	0.2225	0.0674	**0.8567**
	$AUC_{TDBS} \uparrow$	0.0901	0.0484	0.0090	0.0998	0.0175	0.0268	0.1976	0.0514	0.0583	**0.2089**
	$AUC_{ODP} \uparrow$	0.7774	0.6403	0.5214	0.7792	0.4344	0.5760	1.1061	0.6695	0.7477	**1.1370**

Experiments

- Ablation study

Dataset	Without PCA		Without WTNN		Without WMS		Without PnP Prior		WMS-LRTR	
	$AUC_{(D,F)} \uparrow$	Time(s)	$AUC_{(D,F)} \uparrow$	Time(s)	$AUC_{(D,F)} \uparrow$	Time(s)	$AUC_{(D,F)} \uparrow$	Time(s)	$AUC_{(D,F)} \uparrow$	Time(s)
Airport-1	0.9076	14801.741	0.8294	226.314	0.9350	46.210	0.9240	195.416	0.9435	222.551
Airport-2	0.9322	12431.595	0.9585	96.175	0.9627	26.713	0.9441	62.733	0.9704	92.963
Airport-3	0.9274	15124.256	0.9529	271.938	0.9546	132.316	0.9533	179.844	0.9579	297.676
Airport-4	0.9779	13547.221	0.9914	138.498	0.9952	41.520	0.9906	96.701	0.9961	130.514
Average	0.9363	13976.203	0.9331	183.231	0.9619	61.690	0.9530	133.674	0.9670	185.926

- Runtime comparisons

Dataset	RX	LRASR	GTVLRR	AUTO-AD	RGAE	DeCNN-AD	PTA	PCA-TLRSR	LARTVAD	WMS-LRTR
Airport-1	0.102	36.594	214.276	53.080	151.695	56.391	41.515	5.185	46.579	222.551
Airport-2	0.387	52.394	223.684	24.520	144.780	61.706	30.623	5.322	51.808	92.963
Airport-3	0.089	47.754	171.489	20.675	152.961	73.266	36.622	21.625	40.472	297.676
Airport-4	0.092	40.181	180.609	26.694	156.080	77.445	33.261	22.451	55.220	130.514
Average	0.168	44.231	197.515	31.242	151.379	67.202	35.505	13.646	48.520	185.926

Experiments

- Multidirectional analysis

Dataset	Index	H	V	S	M
Airport-1	$AUC_{(D,F)} \uparrow$	0.9428	0.9415	0.9412	0.9435
Airport-2	$AUC_{(D,F)} \uparrow$	0.9679	0.9686	0.9629	0.9704
Airport-3	$AUC_{(D,F)} \uparrow$	0.9547	0.9526	0.9577	0.9579
Airport-4	$AUC_{(D,F)} \uparrow$	0.9958	0.9956	0.9950	0.9961

- Convergence analysis

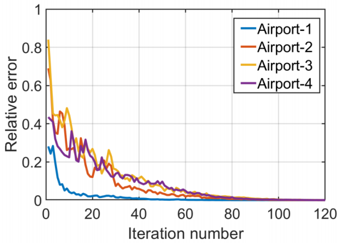

- Block-size analysis

Dataset	Index	2×2	3×3	4×4	5×5
Airport-1	$AUC_{(D,F)} \uparrow$	0.9435	0.9424	0.9379	0.9335
	Time(s)	222.551	240.222	313.199	506.953
Airport-2	$AUC_{(D,F)} \uparrow$	0.9704	0.9663	0.9659	0.9612
	Time(s)	92.963	111.301	132.522	204.909
Airport-3	$AUC_{(D,F)} \uparrow$	0.9579	0.9597	0.9587	0.9595
	Time(s)	297.676	358.482	419.583	494.698
Airport-4	$AUC_{(D,F)} \uparrow$	0.9961	0.9960	0.9953	0.9955
	Time(s)	130.514	150.457	179.795	278.522

Outline

Future Work

- Tuning-free parameter $\Rightarrow$ deep unfolding networks
  - F. Wu, T. Zhang, L. Li, Y. Huang, Z. Peng, RPCANet: Deep Unfolding RPCA Based Infrared Small Target Detection, IEEE/CVF Winter Conference on Applications of Computer Vision, 2024
  - J. Zhang, B. Ghanem, ISTA-Net: Interpretable Optimization-Inspired Deep Network for Image Compressive Sensing, IEEE Conference on Computer Vision and Pattern Recognition, 2018
  - K. Gregor, Y. LeCun, Learning Fast Approximations of Sparse Coding, International Conference on Machine Learning, 2010
- Low complexity $\Rightarrow$ parallel and distributed computing
  - K. Yu, Z. Wu, J. Sun, Y. Zhang, Y. Xu, Z. Wei, Accelerating Hyperspectral Anomaly Detection With Enhanced Multivariate Gaussianization Based on FPGA, IEEE Transactions on Geoscience and Remote Sensing, 2024
  - Q .Du, B. Tang, .W Xie, W. Li, Parallel and Distributed Computing for Anomaly Detection From Hyperspectral Remote Sensing Imagery, Proceedings of the IEEE, 2021
  - J. Lei, G. Yang, W. Xie, Y. Li, X. Jia, A Low-Complexity Hyperspectral Anomaly Detection Algorithm and Its FPGA Implementation, IEEE Journal of Selected Topics in Applied Earth Observations and Remote Sensing, 2020

References

- J. Liu, J. Jin, X. Xiu, W. Liu, J. Zhang, Exploiting Weighted Multidirectional Sparsity for Prior Enhanced Anomaly Detection in Hyperspectral Images, Remote Sensing, 2025
- J. Liu, M. Feng, X. Xiu, X. Zeng, J. Zhang, Tensor Low-Rank Approximation via Plug-and-Play Priors for Anomaly Detection in Remote Sensing Images, IEEE Transactions on Instrumentation and Measurement, 2025

Thank you for your attention!

xcxiu@shu.edu.cn